JOURNAL OF MASS SPECTROMETRY
J. Mass Spectrom. 2008; **43**: 1274–1284
Published online 12 March 2008 in Wiley InterScience
(www.interscience.wiley.com) DOI: 10.1002/jms.1405

JMS

Characterization of Ni(II) complexes of Schiff bases of amino acids and (*S*)-*N*-(2-benzoylphenyl)-1-benzylpyrrolidine-2-carboxamide using ion trap and QqTOF electrospray ionization tandem mass spectrometry

Robert Jirásko,[1] Michal Holčapek,[1]* Lenka Kolářová,[1] Milan Nádvorník[2] and Alexander Popkov[3]

[1] Department of Analytical Chemistry, Faculty of Chemical Technology, University of Pardubice, nám. Čs. legií 565, 532 10, Pardubice, Czech Republic
[2] Department of General and Inorganic Chemistry, Faculty of Chemical Technology, University of Pardubice, nám. Čs. legii 565, 532 10, Pardubice, Czech Republic
[3] Department of Nuclear Medicine and Molecular Imaging, University Medical Center, 9700 RB Groningen, The Netherlands

Received 20 September 2007; Accepted 6 February 2008

This work demonstrates the application of electrospray ionization mass spectrometry (ESI-MS) using two different mass analyzers, ion trap and hybrid quadrupole time-of-flight (QqTOF) mass analyzer, for the structural characterization of Ni(II) complexes of Schiff bases of (*S*)-*N*-(2-benzoylphenyl)-1-benzylpyrrolidine-2-carboxamide with different amino acids. ESI enables the determination of molecular weight on the basis of rather simple positive-ion ESI mass spectra containing only protonated molecules and adducts with sodium or potassium ions. Fragmentation patterns are characterized by tandem mass spectrometric experiments, where both tandem mass analyzers provide complementary information. QqTOF data are used for the determination of elemental composition of individual ions due to mass accuracies always better than 3 ppm with the external calibration, while multistage tandem mass spectra obtained by the ion trap are suitable for studying the fragmentation paths. The novel aspect of our approach is the combination of mass accuracies and relative abundances of all isotopic peaks in isotopic clusters providing more powerful data for the structural characterization of organometallic compounds containing polyisotopic elements. The benefit of relative and absolute mean mass accuracies is demonstrated on the example of studied Ni(II) complexes. Copyright © 2008 John Wiley & Sons, Ltd.

KEYWORDS: amino acid; nickel complex; organometallics; Schiff base; electrospray; QqTOF; ion trap; asymmetric synthesis

INTRODUCTION

Ni(II) complexes of Schiff bases of (*S*)-*N*-(2-benzoylphenyl)-1-benzylpyrrolidine-2-carboxamide and different amino acids are being developed as artificial analogs of pyridoxal 5′-phosphate (PLP) dependent enzymes.[1] Their preparative applications for stoichiometric asymmetric synthesis of α-amino acids have been optimized by a number of groups worldwide.[2–6] These complexes are also precursors for helically chiral nanomaterials.[7] The scheme of their preparation is shown in Fig. 1. This reaction promotes mainly the formation of *S*,*S*-diastereomer due to thermodynamic control of stereochemistry of the newly created asymmetric center.[8,9] The preparation of peptide analogs stable toward proteases is a versatile approach in the development of peptidomimetic drug candidates. They can also be used as conformationally restricted models of natural peptides for nuclear magnetic resonance (NMR), circular dichroism, and crystallographic investigations.[10] For positron emission tomography,[10,11] β^+-emitting radiopharmaceuticals can be prepared by the introduction of labeled ^{11}C-methyl group by the reaction of a particular complex of α-amino acid with labeled $^{11}CH_3I$ or by alkylation with a ^{18}F-bearing benzyl-halogenide. In case of amino acid containing nucleophilic heteroatoms in its side chain, such as tryptophan (nitrogen) and tyrosine (oxygen), the methylation could take place on these heteroatoms instead of desired α-carbon of amino acid. Therefore, it is necessary to protect heteroatoms using a suitable protective group, e.g. tert-butyl or tert-butyl carbamate (Boc) protective groups. Chiral synthons of α-amino acids labeled with ^{13}C or ^{15}N are useful tools in the preparation of α-amino acids that are enantiomerically pure and selectively isotopically substituted for NMR and MS studies of biological systems.[12] The established method used for the structure

*Correspondence to: Michal Holčapek, Department of Analytical Chemistry, Faculty of Chemical Technology, University of Pardubice, nám. Čs. legií 565, 532 10, Pardubice, Czech Republic.
E-mail: Michal.Holcapek@upce.cz

elucidation of organonickel compounds is NMR based on ^{1}H and ^{13}C chemical shifts.[13,14] When a single crystal can be prepared, then X-ray is a method of choice[9,15] due to the highest solid-state structural information content, but on the other hand the preparation of a single crystal may be time-consuming or impossible in some cases.

Electrospray ionization (ESI) is the most suitable ionization technique for the analysis of various metal complexes with amino acids and small peptides; for example Cu(II),[16,17] Fe(II),[17] or Ni(II)[18] complexes can be used for differentiation of positional isomers (leucine *vs* isoleucine),[16] diastereoisomers,[17] and chiral isomers.[18] Studies of copper complexes have been published in numerous works,[19–31] but this is the first work devoted exclusively to Ni(II) complexes of amino acids using ESI-MS. Only one previous work of similar Ni(II) was based on matrix-assisted laser desorption/ionization (MALDI), where the ionization and fragmentation behavior shows some differences comparing to present work.[32] The ion trap analyzer is ideally suited for fragmentation pattern studies,[17] while the benefit of time-of-flight (TOF)-based mass analyzers[32] is mainly in the high-resolution and high mass accuracy applicable for the structure elucidation and reliable elemental composition determination. Based on our previous works dealing with the characterization of organotin compounds using ion trap ESI-MS,[33–35] we have applied a combination of both ion trap and hybrid quadrupole time-of-flight (QqTOF) mass analyzer for the structure elucidation of amino acid nickel complexes providing complementary data. Moreover, the fragmentation behavior is compared with previous studies of Cu(II) complexes of amino acids to look for both similarities and differences.

EXPERIMENTAL

Ni(II) complexes of Schiff bases of (*S*)-*N*-(2-benzoylphenyl)-1-pentamethylbenzylpyrrolidine-2-carboxamide and glycine or (^{15}N)glycine were prepared using a standard procedure previously described for similar complexes derived from nonpentamethylated (*S*)-*N*-(2-benzoylphenyl)-1-benzylpyrrolidine-2-carboxamide and glycine or (^{15}N)glycine.[12] The compounds were fully characterized by ^{1}H-NMR, ^{13}C-NMR, and tandem mass spectrometric techniques. Their structures and scheme of preparation are shown in Fig. 1. Possible structures of methylation products (explained in Results and Discussion) are shown in Fig. 2. These compounds provided a signal only in the positive-ion ESI-MS mode and they were characterized using two different tandem mass spectrometers.

(1) Ion trap analyzer (Esquire 3000, Bruker Daltonics, Germany) – the mass spectra were measured in the range m/z 50–1000. The samples were dissolved in acetonitrile and analyzed by direct infusion at a flow rate of 5 µl/ min. The ion source temperature was 300 °C; the flow rate and the pressure of nitrogen were 4 l/min and 10 psi, respectively. The selected precursor ions were further analyzed by MS/MS analyses under the following conditions: the isolation width $\Delta m/z$ 6 and the collision amplitude in the range 0.8–0.9 V depending on the precursor ion stability.

(2) Hybrid QqTOF analyzer (micrOTOF-Q, Bruker Daltonics, Germany) – the mass spectra were measured in the range m/z 50–1000. The instrument was externally calibrated using ESI tuning mix before the individual measurements. The samples were dissolved in acetonitrile and analyzed by direct infusion at a flow rate of 3 µl/ min. Interface parameters were set as follows: capillary voltage = −4.5 kV, drying temperature = 200 °C; the flow rate and pressure of nitrogen were 4 l/min and 0.4 bar, respectively. Data were acquired by summation of 50 000 scans with 10 rolling averages for 2 min to obtain the accurate masses. The collision energy for tandem mass spectra measurements was set in the range 25–30 eV/z.

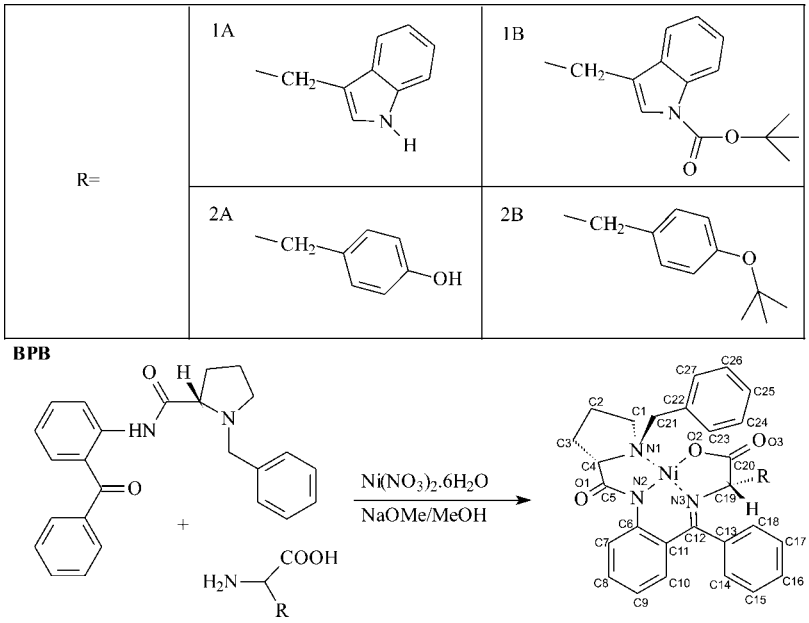

Figure 1. Structures of studied compounds and the reaction scheme of their preparation.

DOI: 10.1002/jms

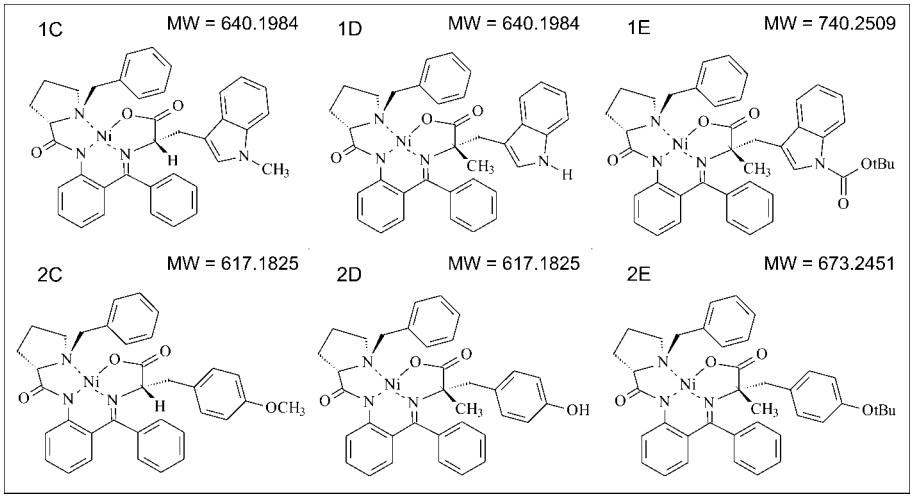

Figure 2. Possible structures of methylation products for protected tryptophan (**1**) and tyrosine (**2**) complexes.

For the confirmation of proposed fragmentation paths, other labeled complexes were synthesized and analyzed by MS/MS: ^{15}N3, ^{13}C19, and ^{13}C20. All measurements were repeated in perdeuterated methanol (CD_3OD) to obtain deuterated molecule $[M + D]^+$ for easier localization of protonation (deuteration) site. The same was also done with $[M + Na]^+$ ions.

RESULTS AND DISCUSSION

Protonated molecules $[M + H]^+$ and adducts with alkali metal ions $[M + Na]^+$ and $[M + K]^+$ are observed in the full scan positive-ion ESI mass spectra for both analyzers (Fig. 3). The main difference between these spectra is the resolution and mass accuracy, both of which are much better for QqTOF analyzer (Table 1). The exact evaluation of experimental isotopic distribution and the comparison with theoretical data is a useful tool in the mass spectra interpretation of polyisotopic elements such as tin,[34,35] germanium,[36] nickel, and many others because polyisotopic elements significantly contribute to the total isotopic distribution. This approach can reveal their presence or absence in the structure of individual ions. The comparison of theoretical and experimental isotopic distributions is shown in Fig. 4 on the example of $[M + H]^+$ ion for compound **1A**. All data obtained with both analyzers provide a very good fit with theoretical isotopic patterns. Due to high mass accuracy of QqTOF analyzer, we evaluated all isotopic masses and obtained mass errors (mass accuracies) for all isotopic peaks (m/z_{exp}) by the comparison with theoretical calculated exact masses (m/z_{theor}).

$$Mass\ error = mass\ accuracy = 10^6 \times \frac{m/z_{exp} - m/z_{theor}}{m/z_{theor}} \quad (1)$$

Further, absolute and relative mean mass errors are calculated which is the intensity (I_i) weighted mean absolute or relative deviation (err_i) between measured masses and theoretical masses of all peaks (n is the number of isotopes).

$$Absolute\ mean\ mass\ error = \frac{|err_1| \times I_1 + |err_2| \times I_2 + \cdots + |err_n| \times I_n}{\sum_{i=1}^{n} I_i} \quad (2)$$

It is worthy to point out the difference between the relative and absolute mean mass accuracies. The relative mean mass accuracy is calculated as the mean of mass accuracies of all isotopes including plus/minus sign, while the absolute mean mass accuracy is the mean of absolute values of mass accuracies. Let us suppose a simple example of isotopic distribution containing only two ions with mass accuracies +3 and −3 ppm; then the relative mean mass accuracy is 0 ppm, while the absolute mean mass accuracy is 3 ppm. Each parameter has different information content; the relative value should have very low values on the condition that the mass calibration is precise, without a systematic error and real mass errors have random distribution. On the other hand, the absolute mean mass accuracy is the average difference between theoretical and experimental m/z values not regarding the sign; therefore much lower convergence to zero is expected. In general, worse accuracies may be expected for low abundant isotopic peaks, which are treated by considering the relative abundances in the calculation algorithm. Both mean values can be strongly affected by the overlap with interfering ions, as discussed later in the example of $[M + Na]^+$ of **2E**.

A sigma value is used for individual ions as the combined value of the standard deviation of relative abundances for all peaks in the isotopic cluster from theoretical values.[37] The correct determination of the elemental composition of individual ions is even more reliable, when all isotopes considering their relative abundances are taken into account comparing the established approach using only the most abundant isotopic ion. Typically, the sigma values lower than 0.05 predict the possibility of correct hit; mostly experimental sigma values are bellow 0.02 for the right elemental composition. On the other hand, values higher than 0.10 are considered as a strong indication that the suggested elemental composition is not correct or the interference is present. In our case, the worst mean mass accuracy of sodium molecular adduct with theoretical monoisotopic mass m/z 696.2343 for compound **2E** is caused by the interference of the isotopic peak M + 2 with monoisotopic mass m/z 698.1926 corresponding to the potassium molecular adduct of compound **2B**. The resolution deducted from the spectrum

DOI: 10.1002/jms

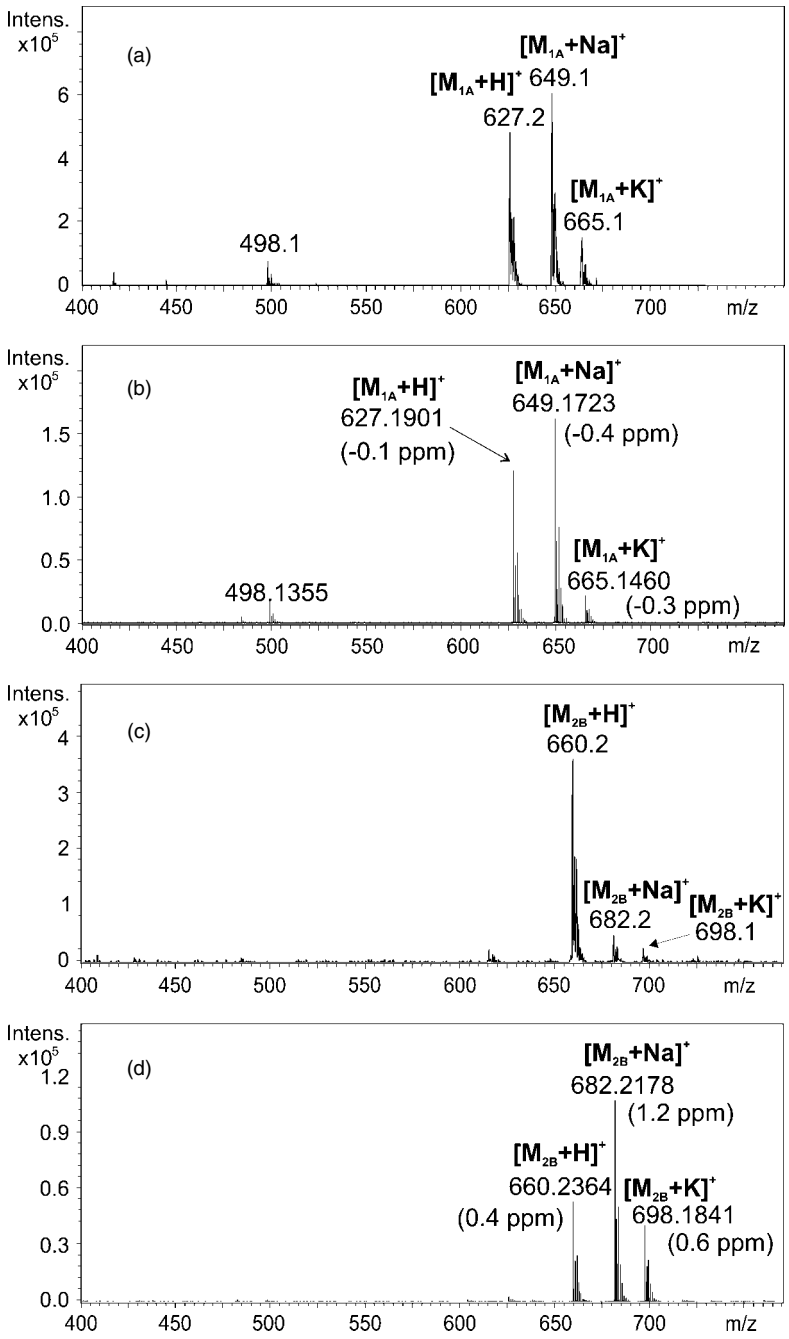

Figure 3. Full scan positive-ion ESI mass spectra: (a) ion trap spectrum of compound **1A**, (b) QqTOF spectrum of compound **1A**, (c) ion trap spectrum of compound **2B**, (d) QqTOF spectrum of compound **2B**.

(Fig. 5) is equal to 11 721 which is deficient to resolve these two ions and hence only an envelope formed by the superposition of particular isotopes shifting the correct mass is observed. However, the mass accuracy of the first and second isotopes for $[M_{2E} + Na]^+$ is below 1 ppm (0.7 and 0.3 ppm), because the isotopic distribution is affected by superposition of $[M_{2B} + K]^+$ starting from the third isotope (m/z 698.2320).

The presence or absence of a protective group on the aromatic nitrogen (for tryptophan) or oxygen (for tyrosine) is easily recognized based on the determination of the molecular weights. Furthermore, the presence of a protective group is confirmed by typical neutral losses associated with this group ($\Delta m/z$ 56 for butene or $\Delta m/z$ 100 for Boc protective group) observed in tandem mass spectra of $[M + H]^+$ (Fig. 6). The abundant ion at m/z 498 formed by the loss of stable conjugated system $\Delta m/z$ 129 is an indication of tryptophan complex or $\Delta m/z$ 106 of tyrosine complex (see Fig. 6 for structures of neutral losses in agreement with[19]). This ion is also the base peak in MS/MS spectra of nonprotected complexes and its structure is basically similar to the protonated molecule of glycine complex which was confirmed by the measurement of tandem mass spectra of glycine complex. The facile elimination of tryptophan (Fig. 6(a,b)) and tyrosine (Fig. 6(c,d)) side chains is similar as reported recently for ternary Cu(II) complexes.[20,21,24] Tandem mass spectra on both analyzers show identical ions only differing in their relative abundances. The measurement of multistage mass spectra

DOI: 10.1002/jms

Table 1. Theoretical masses, mass accuracy, relative mean mass accuracy, absolute mean mass accuracy, and sigma value for deprotonated molecules, sodium and potassium molecular adducts for all studied compounds (values are in ppm except for sigma)

		$[M+H]^+$	$[M+Na]^+$	$[M+K]^+$
Compound **1A**	Theoretical m/z	627.1901	649.1720	665.1459
	Mass accuracy	−0.1	−0.4	−0.3
	Relative mean mass accuracy	−0.2	−0.3	−1.3
	Absolute mean mass accuracy	0.6	0.5	1.7
	Sigma	0.015	0.009	0.027
Compound **1B**	Theoretical m/z	727.2425	749.2244	765.1984
	Mass accuracy	2.6	2.4	0.9
	Relative mean mass accuracy	2.3	1.8	1.0
	Absolute mean mass accuracy	2.3	1.7	1.0
	Sigma	0.010	0.008	0.018
Compound **1C**	Theoretical m/z	641.2057	663.1877	679.1616
	Mass accuracy	−0.9	0.0	−3.2
	Relative mean mass accuracy	−1.0	0.5	−2.5
	Absolute mean mass accuracy	1.0	0.7	2.6
	Sigma	0.013	0.012	0.020
Compound **2A**	Theoretical m/z	604.1741	626.1560	642.1300
	Mass accuracy	−2.6	−1.1	−2.3
	Relative mean mass accuracy	−2.5	−1.8	−1.6
	Absolute mean mass accuracy	2.6	1.9	2.3
	Sigma	0.023	0.008	0.021
Compound **2B**	Theoretical m/z	660.2367	682.2186	698.1926
	Mass accuracy	0.4	1.2	0.6
	Relative mean mass accuracy	0.1	0.7	0.2
	Absolute mean mass accuracy	0.6	0.7	0.6
	Sigma	0.014	0.011	0.013
Compound **2E**	Theoretical m/z	674.2523	696.2343	712.2082
	Mass accuracy	−0.5	−0.7	0.2
	Relative mean mass accuracy	−0.5	7.2[a]	−0.4
	Absolute mean mass accuracy	0.5	9.2[a]	0.9
	Sigma	0.004	0.045[a]	0.019

[a] Partial overlap with non-resolved $[M+K]^+$ ion of **2B**.

on the ion trap analyzer provides more structural information for studying the fragmentation paths (Fig. 7(a–c)), as illustrated in the fragmentation scheme of ion at m/z 498 suggested on the basis of a detailed interpretation of MS^n spectra (Fig. 8). All suggested fragmentation paths are confirmed by the measurement of individual MS^n spectra step by step. All observed ions are singly charged, some of them are radical ions, as indicated in this figure.

The QqTOF analyzer enables mass spectra measurements only up to MS^2. The formation of fragment ions in MS/MS spectra depends on the collision induced dissociation (CID) which may be also performed in the source without the isolation step (in-source CID). When the in-source CID energy value is increased from 0 to 150 eV/z, then the peaks corresponding to $[M+H]^+/[M-H]^-$ ions have reduced relative abundances at the cost of increased relative abundances of product ions (e.g. m/z 498). Subsequently, MS/MS spectrum of m/z 498 can be recorded. The overall appearance of this spectrum is very close to the ion trap MS^3 spectrum (Fig. 7(d)), but provides high mass accuracy applicable for the elemental composition determination.

Further, the methylation of protected complexes has been performed. Figure 2 shows three possible products which may be formed by the methylation. The structures **1E** and **2E** correspond to the situation when the protective group

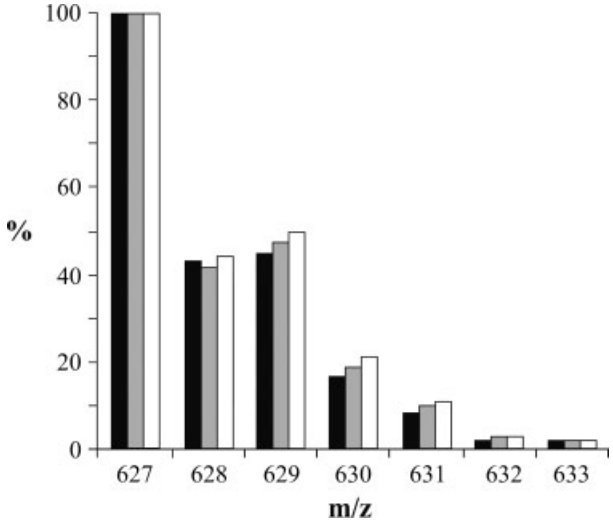

Figure 4. Comparison of experimental (ion trap – black bars, QqTOF – gray bars) and theoretical (white bars) isotopic abundances for protonated molecule of compound **1A**.

DOI: 10.1002/jms

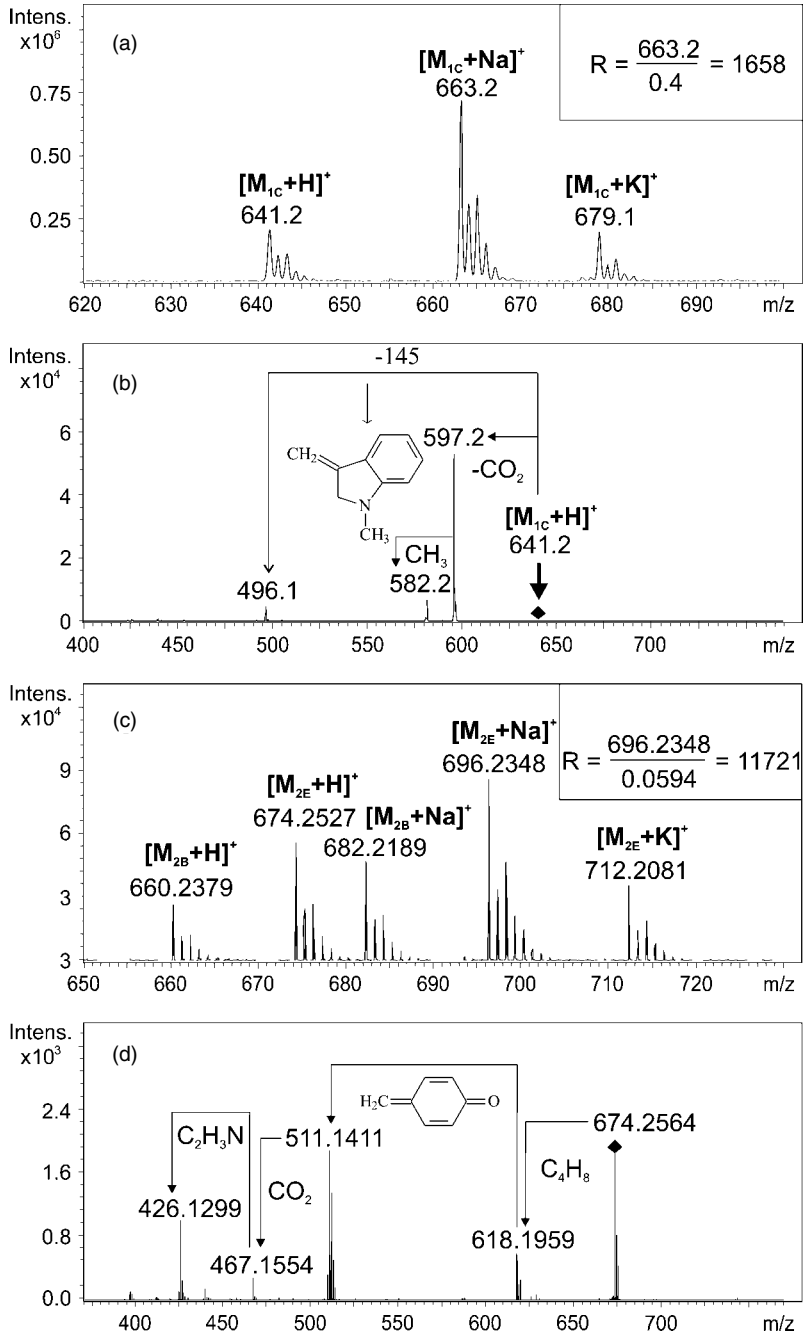

Figure 5. (a) Zoom of ion trap full scan positive-ion ESI mass spectra for methylation product **1C** with the calculated resolution, (b) Tandem mass spectrum of protonated molecule of **1C** (collision energy 0.8 V; isolation width $\Delta m/z$ 6), (c) Zoom of QqTOF full scan positive-ion ESI mass spectra for methylation product **2E** with the calculated resolution, (d) Tandem mass spectrum of protonated molecules of **2E** (collision energy 25 eV/z; isolation width $\Delta m/z$ 6).

is still present on the heteroatoms and the methylation is successfully carried out on desired α-methyl carbon of amino acids. However, during harsh conditions of methylation procedure, the complex may be deprotected and the methyl group can attack the heterocyclic nitrogen or oxygen (structures **1C** and **2C**). The last hypothetical possibility is that the complex is deprotected but the methylation is still successful (structures **1D** and **2D**). Mass spectrometric results make possible to exactly describe the reaction course of methylation, which is reported for the first time. It is evident from ions observed in the full scan positive-ion mass spectrum of methylated tryptophan complex (Fig. 5(a)) that the complex is deprotected. Two structural possibilities with different methyl location still remain. Due to the same molecular weights, it is impossible to reveal the correct one based on the molecular weights only. It is necessary to search for the diagnostic product ions in MS/MS to distinguish between two possibilities. The MS/MS spectrum of protonated molecule at m/z 641 is shown in Fig. 5(b). In case of methyl group bonded to the desired α-carbon of amino acid, the side chain of the complex is identical as for compound **1A**. The supposed neutral loss of this complex would be probably formed also by the loss of very stable conjugated system corresponding to $\Delta m/z$ 129.

DOI: 10.1002/jms

JMS

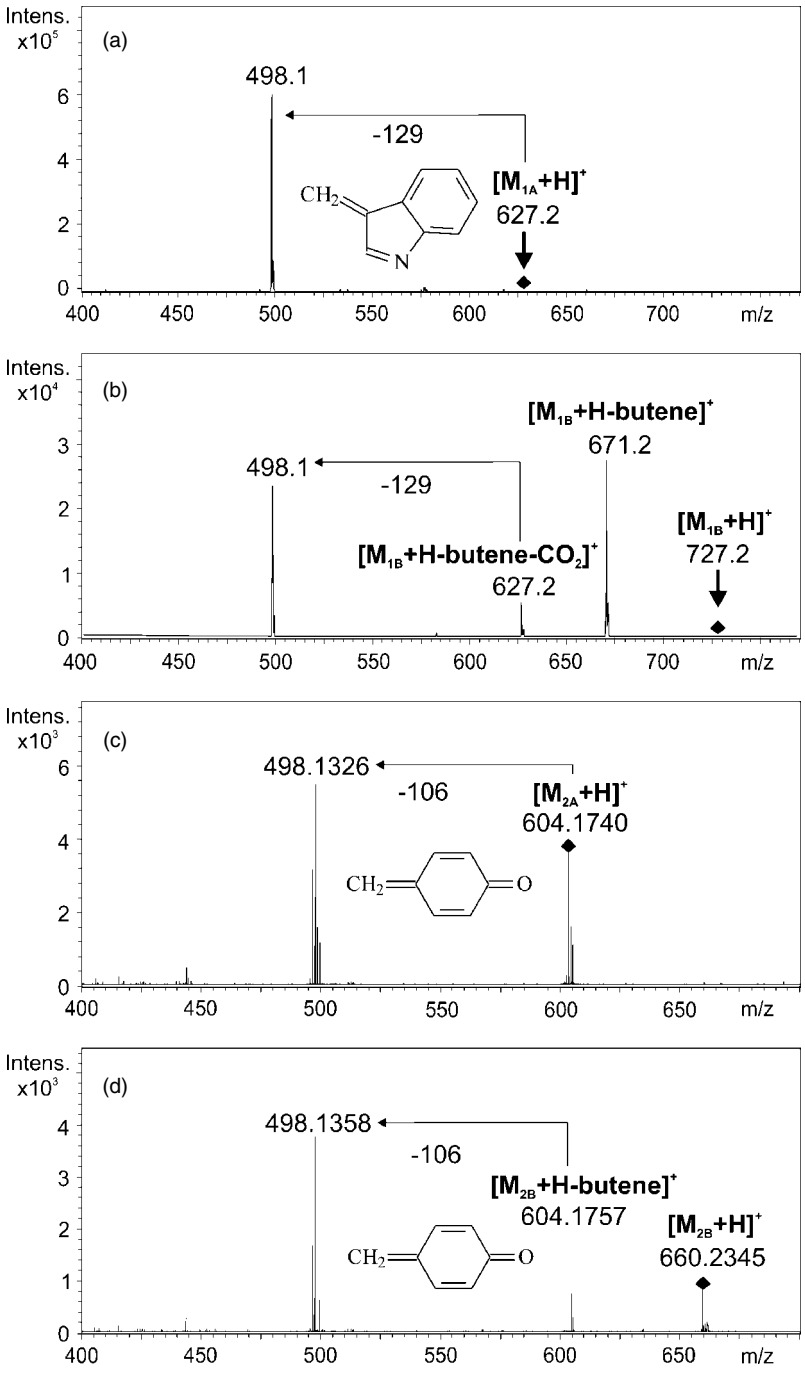

Figure 6. Tandem mass spectra of protonated molecules: (a) ion trap spectrum of compound **1A** (collision energy 0.8 V; isolation width $\Delta m/z$ 6), (b) ion trap spectrum of compound **1B** (collision energy 0.9 V; isolation width $\Delta m/z$ 6), (c) QqTOF spectrum of compound **2A** (collision energy 25 eV/z; isolation width $\Delta m/z$ 6), (d) QqTOF spectrum of compound **2B** (collision energy 30 eV/z; isolation width $\Delta m/z$ 6).

However, the different neutral losses (CO_2 and $\Delta m/z$ 145) are observed in the spectra, which are explained by the fact that the formation of stable conjugated system is affected by the presence of methyl group on the nitrogen and then the neutral loss of carbon dioxide is preferred. Second, the loss of $\Delta m/z$ 145 is explained by the loss of the side chain of **1C** (Fig. 2). Consequently, it can be concluded that methylation has occurred in the nitrogen atom. Under harsh reaction conditions of methylation, the compounds are deprotected and the methylation leads to pure N-methylated products without any traces of C-methylation.

In the case of the complex derived from O-methylated tyrosine, the protective group is stable enough and ions corresponding to C-methylated product are accompanied by ions of protected tyrosine complex without methylation (i.e. starting compound) in the full scan positive-ion spectra (Fig. 5(c)). The elemental composition is confirmed by QqTOF data. MS/MS spectrum of $[M_{2E} + H]^+$ ion provides information about successful methylation (Fig. 5(d)). The neutral loss associated with the presence of methyl group on the heteroatom (oxygen) is not observed. First, the neutral loss of protective tert-butyl group is found. However,

DOI: 10.1002/jms

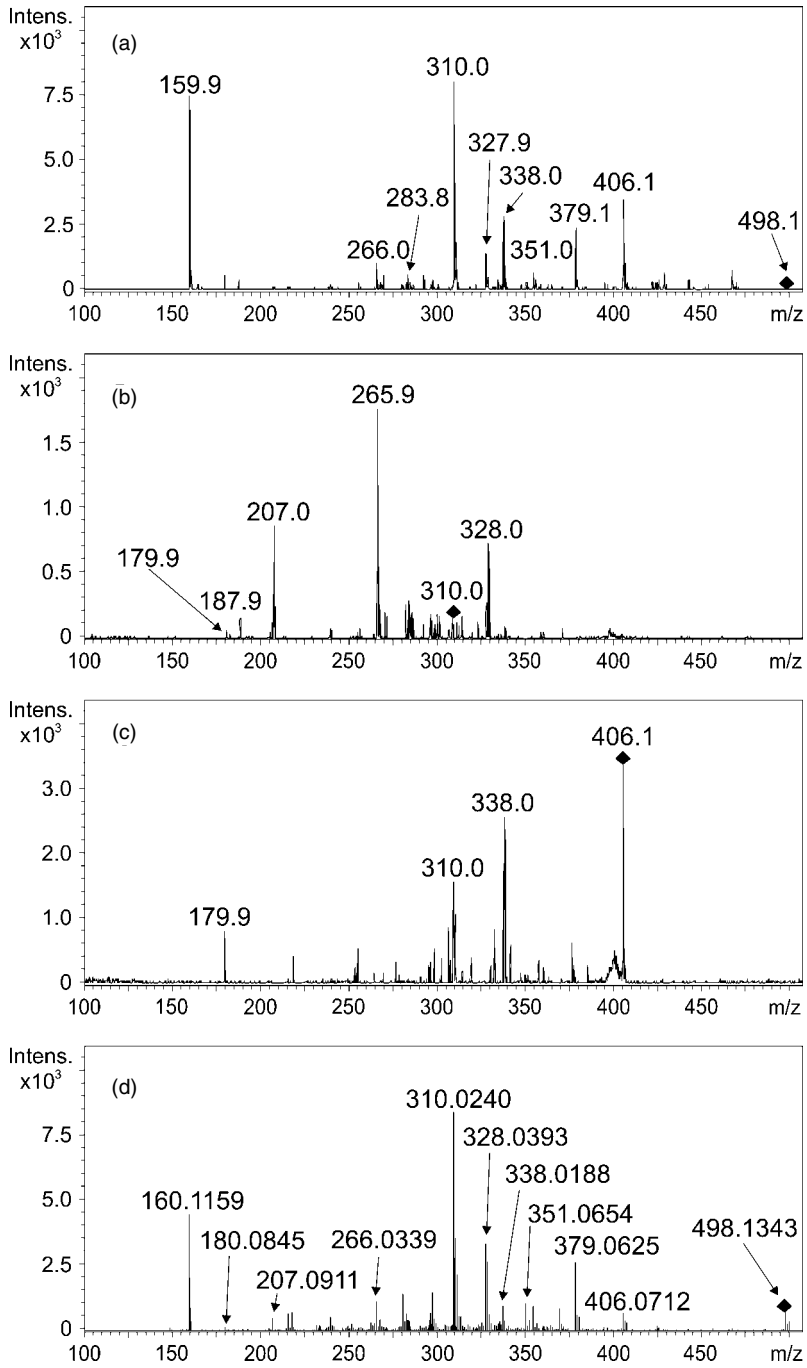

Figure 7. Tandem mass spectra of compound **1A**: (a) ion trap MS^3 spectrum of fragmentation path *m/z* 627–498 (collision energy 0.8 V; isolation width $\Delta m/z$ 6), (b) ion trap MS^4 spectrum of fragmentation path *m/z* 627–498–310 (collision energy 0.8 V; isolation width $\Delta m/z$ 6), (c) ion trap MS^4 spectrum of fragmentation path *m/z* 627–498–406 (collision energy 0.8 V; isolation width $\Delta m/z$ 6), (d) QqTOF in-source collision induced dissociation followed by MS^2 spectrum of *m/z* 498 (collision energy 30 eV/z; isolation width $\Delta m/z$ 6). Suggested structures of observed ions are shown in the fragmentation scheme in Fig. 8.

presence of methyl on the desired α-methyl carbon of amino acid leads to the formation of radical ion at m/z 511 by the loss of $\Delta m/z$ 107 in comparison to nonmethylated tyrosine complex with $\Delta m/z$ 106. The losses of carbon dioxide and C_2H_3N are also recognized in the spectrum probably due to the presence of methyl group. Based on the above-mentioned interpretation, the success of α-methylation is confirmed (Fig. 2 – structure **2E**).

The elemental composition of all ions and all neutral losses shown in Fig. 8 were clearly confirmed by high mass accuracy measurements to avoid any speculation in cases of more potential interpretations, e.g. neutral losses of CO *versus* CH_2CH_2. To confirm the proposed fragmentation scheme, several independent experiments were performed: (1) measurements in perdeuterated solvent (i.e. CD_3OD) to obtain $[M + D]^+$ because of better localization of protonation site in subsequent MS^n experiments, (2) MS^n of $[M + Na]^+$ ion, (3) MS^n of three isotopically labeled standards in the following positions $^{15}N3$, $^{13}C19$, and $^{13}C20$ for the confirmation of suggested fragmentation scheme. The

DOI: 10.1002/jms

JMS

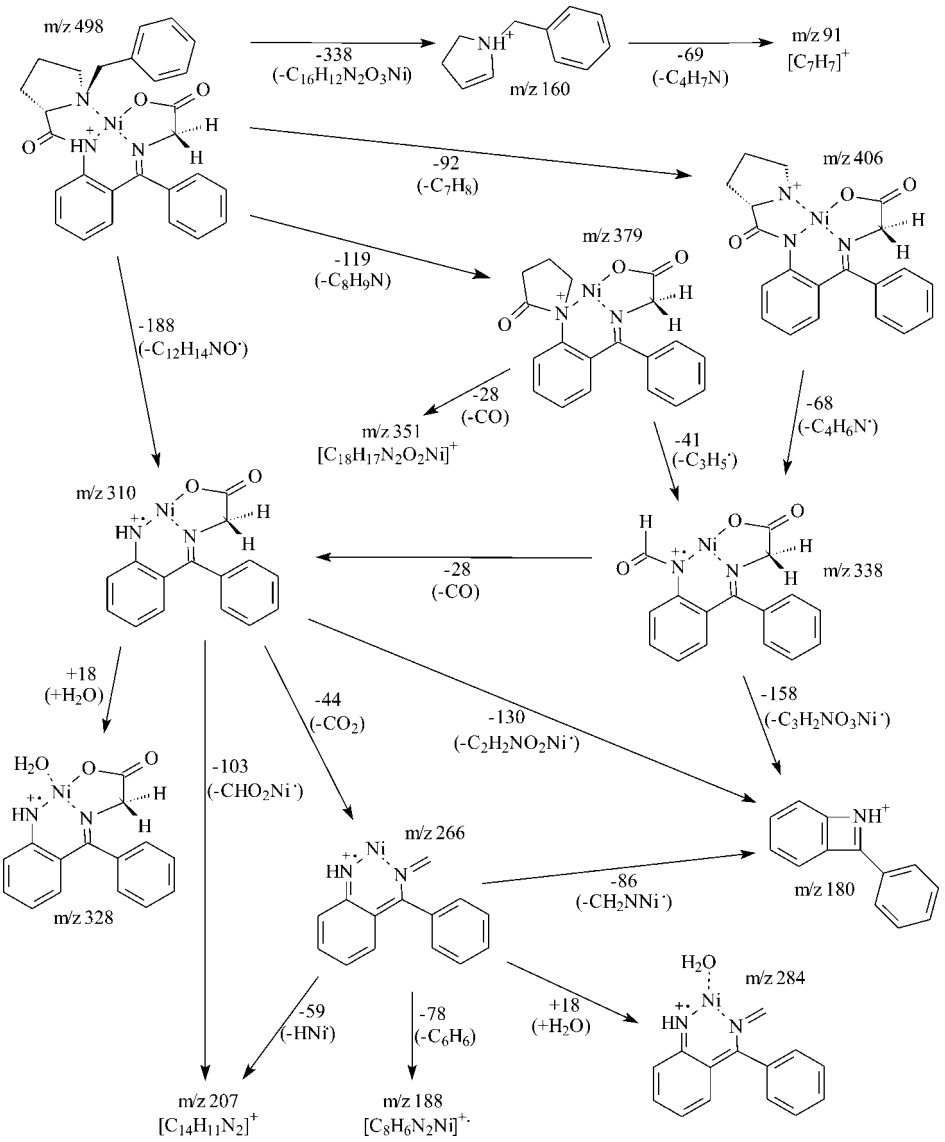

Figure 8. Suggested fragmentation pattern of $[M + H]^+$ ion at *m/z* 498 based on ion trap ESI-MS^n analysis and QqTOF verification of accurate masses for compound **1A**.

localization of the most probable protonation site is based on the comparison of MS^n of $[M + D]^+$ with nonlabeled compound. The mass shift +1 related to one deuterium is observed for the following ions and their products: *m/z* 406, 379, 338, 328, 310, and 266. On the other hand, no change is observed for *m/z* 160 and 91. Considering that the protonation should be placed on the most basic center in the molecule, two reasonable possibilities still remain: nitrogen atoms N2 and N3 (see numbering in Fig. 1). These possibilities can be distinguished with the help of the product ion *m/z* 180 containing only N2 and is clearly shifted to *m/z* 181 which suggests that the most probable protonation site is at N2, as indicated in Fig. 8. The question whether the ion *m/z* 180 really contains N2 but not N3 is answered by the measurement of ^{15}N3 labeled standard, where the loss of labeled ^{15}N3 is observed in the fragmentation step from *m/z* 267 to 180. The experiment with MS^n of $[M + Na]^+$ ion provided comparable results as for $[M + D]^+$, i.e. no shift for *m/z* 160 and 91 and a mass shift of *m/z* 22 units for ions *m/z* 406, 310, 338, 266, and 207. Some less abundant ions (*m/z* 379, 328, 284, and 180) were not detected in this experiment with $[M + Na]^+$ because of sensitivity limitation with the sodium adduct. It seems probable that sodium adduct formation also takes place at N2, but there is no experimental proof to reject the second alternative of N3 because of the lack of sensitivity.

MS^n experiments with three labeled standards at positions ^{15}N3, ^{13}C19, and ^{13}C20 confirmed that all ions proposed in Fig. 8 are in agreement with these spectra. Nitrogen ^{15}N3 is present in ions at *m/z* 406, 338, 328, 310, 284, 266, 207, and absent in ions *m/z* 180, 160, and 91. Carbon ^{13}C19 is observed in ions at *m/z* 406, 338, 328, 310, 284, 266, 207, and absent in *m/z* 180, 160, and 91. Carbon ^{13}C20 is detected only in the following ions: *m/z* 406, 338, 328, and 310. The important information is that ^{13}C20 is retained in the structure during the loss of CO from *m/z* 338 to 310, but it is lost in the fragmentation step from *m/z* 310 to 266 corresponding to the neutral loss of CO_2 in agreement with Fig. 8.

The typical feature of ESI mass spectra of Cu(II) complexes with amino acids[25–27] and small peptides[28,29] is the formation of radical ions which may then be used for the

DOI: 10.1002/jms

generation of radical ion of amino acid itself for further gas-phase studies.[19–24] The behavior is less pronounced in the case of Ni(II), which may be explained by the fact that copper has two common oxidation states Cu(II)/Cu(I) and hence it exhibits redox properties unlike Ni(II) with only one common oxidation state Ni(II). The radical ions in the spectra of Ni(II) are apparent only in MS^n spectra but not for ions in the molecular region. In some cases, the even electron ion is accompanied by a radical ion with lower relative intensity, for example the base peak m/z 498 in Fig. 6(c and d) is accompanied by the radical at m/z 497 with relative intensities 57 and 44%, respectively. The only logical explanation of the formation of m/z 497 is the radical loss of tyrosine side chain from $[M_{2A} + H]^+$ in Fig. 6(c) and from $[M_{2B} + H\text{-butene}]^+$ in Fig. 6(d). The interesting difference is between ion trap (Fig. 6(a,b)) and QqTOF (Fig. 6(c,d)) MS/MS spectra because the radical ion m/z is completely missing in the ion trap spectra, while it has notable abundances in QqTOF spectra that may probably be caused by longer reaction time in the trap (milliseconds) in comparison to QqTOF (microseconds).

The addition of small neutral species containing oxygen to the fragment ion in the trap after the loss of the substituent bonded to the central metal atom is already known from the previous study of other organometallic complexes, where the addition of O_2 complemented two lost substituents on the central Co(III) atom.[38] In our case, the radical ion m/z 310 formed by the loss of the radical side chain on the central Ni(II) atom is replaced by the addition of H_2O during the isolation of this ion in the trap. A similar example is the path from m/z 266 to 284.

CONCLUSIONS

The complementary information from tandem mass spectra measured by two analyzer types, ion trap and QqTOF, is used for the structural characterization of Ni(II) complexes with Schiff bases of amino acids. The advantage of high-resolution QqTOF analyzer is the determination of accurate m/z values with mass accuracies better than 3 ppm even with the external calibration, which is sufficient for the unambiguous determination of elemental composition and also for the true isotopic pattern recognition. Our approach implements the use of mass accuracies and relative abundances of all isotopes in the isotopic clusters containing a metal element. This combined information about all isotopes (i.e. relative and absolute mean mass accuracies) gives more reliable data in comparison to the conventional approach based on the most abundant isotopic peak only. Other supplementary information is the comparison of theoretical and experimental isotopic patterns for all proposed elemental combinations expressed as the sigma value. The ion trap analyzer is useful for the verification of the presence of polyisotopic elements and mainly for multistage tandem mass spectra measurements important for understanding the whole fragmentation patterns. The presented comprehensive approach is worthy especially in the structural analysis of molecules containing complex polyisotopic elements (e.g. metals), but in principle it is applicable for any organic, bioorganic, and organometallic species.

Acknowledgements

This work was supported by the projects MSM0021627502 sponsored by the Ministry of Education, Youth and Sports of the Czech Republic and 203/08/1536 sponsored by the Czech Science Foundation is acknowledged. M.N. acknowledges the support of the project VZ0021627501 sponsored by the Ministry of Education, Youth and Sports of the Czech Republic.

REFERENCES

1. Belokon YN. Chiral complexes of Ni(II), Cu(II) and Cu(I) as reagents, catalysts and receptors for asymmetric-synthesis and chiral recognition of amino acids. *Pure Appl. Chem.* 1992; **64**: 1917.
2. Debache A, Collet S, Bauchat P, Danion D, Euzenat L, Hercouet A, Carboni B. Belokon's Ni(II) complex as a chiral masked glycine for the diastereoselective synthesis of 2-substituted 1-aminocyclopropane carboxylic acids. *Tetrahedron: Asymmetr.* 2001; **12**: 761.
3. Soloshonok VA, Cai C, Yamada T, Ueki H, Ohfune Y, Hruby VJ. Michael addition reactions between chiral equivalents of a nucleophilic glycine and (S)- or (R)-3-[(E)-Enoyl]-4-phenyl-1,3-oxazolidin-2-ones as a general method for efficient preparation of beta-substituted pyroglutamic acids. Case of topographically controlled stereoselectivity. *J. Am. Chem. Soc.* 2005; **127**: 15296.
4. Vadon-Legoff S, Dijols S, Mansky D, Boucher JL. Improved and high yield synthesis of the potent arginase inhibitor: 2(S)-amino-6-boronohexanoic acid. *Org. Process Res. Dev.* 2005; **9**: 677.
5. Saghiyan AS, Geolchanyan AV. Asymmetric synthesis of all possible stereomers of 4-aminoglutamic acid via Michael condensation of chiral Ni(II) complexes of glycine and dehydroalanine. *Synth. Commun.* 2006; **36**: 3667.
6. Saghiyan AS, Dadayan SA, Petrosyan SG, Manasyan LL, Geolchanyan AV, Djamgaryan SM, Andreasyan SA, Maleev VI, Khrustalev VN. New chiral Ni-II complexes of Schiff's bases of glycine and alanine for efficient asymmetric synthesis of α-amino acids. *Tetrahedron: Asymmetr.* 2006; **17**: 455.
7. Soloshonok VA, Ueki H. Design, synthesis, and characterization of binuclear Ni(II) complexes with inherent helical chirality. *J. Am. Chem. Soc.* 2007; **129**: 2426.
8. Belokon YN, Bakhmutov VI, Chernoglazova NI, Kochetkov KA, Vitt SV, Garbalinskaya NS, Belikov VM. General method for the asymmetric synthesis of α-amino acids via alkylation of the chiral nickel(II) Schiff base complexes of glycine and alanine. *J. Chem. Soc, Perkin Trans. 1* 1988; **2**: 305.
9. Gu XY, Ndungu JA, Qiu W, Ying J, Carducci MD, Wooden H, Hruby VJ. Large scale enantiomeric synthesis, purification, and characterization of ω-unsaturated amino acids via a Gly-Ni(II)-BPB-complex. *Tetrahedron* 2004; **60**: 8233.
10. Popkov A, Nádvorník M, Kružberská P, Lyčka A, Lehel S, Gillings NM. Towards stereoselective radiosynthesis of α-[^{11}C] methylsubstituted aromatic α-amino acids – a challenge of creation of quaternary asymmetric centre in a very short time. *J. Labelled Compd. Radiopharm.* 2007; **50**: 374.
11. Antoni G, Kihlberg T, Långström B. In *Aspects on the Synthesis of ^{11}C-Labelled Compounds (in Handbook of Radiopharmaceuticals)*., Welch MJ, Redvanly CS (eds). Wiley: Chichester, 2003; 141.
12. Nádvorník M, Popkov A. Improved synthesis of the Ni(II) complex of the Schiff base of (*S*)-2-[*N*-(*N*′-benzylprolyl)amino]benzophenone and glycine. *Green Chem.* 2002; **4**: 71.
13. Popkov A, Gee A, Nádvorník M, Lyčka A. Chiral nucleophilic glycine and alanine synthons: nickel(II) complexes of Schiff bases of (*S*)-*N*-(2,4,6-trimethylbenzyl)proline (2-benzoylphenyl)amide and glycine or alanine. *Transit. Metal Chem.* 2002; **27**: 884.
14. Popkov A, Langer V, Manorik PA, Weidlich T. Long-range spin-spin interactions in the C-13-n.m.r. spectra of the nickel(II) complex of the Schiff base of (*S*)-*N*-benzylproline (2-benzoylphenyl)amide and glycine. Quantum-chemical calculations and possible donation of electron density from the π-system of the benzyl group to nickel. *Transit. Metal. Chem.* 2003; **28**: 475.

15. Langer V, Popkov A, Nádvorník M, Lyčka A. Two new Ni(II) Schiff base complexes: X-ray absolute structure determination, synthesis of a ^{15}N-labelled complex and full assignment of its ^{1}H NMR and ^{13}C NMR spectra. *Polyhedron* 2007; **26**: 911.
16. Vaisar T, Gatlin CL, Rao RD, Seymour JL, Tureček F. Sequence information, distinction and quantitation of C-terminal leucine and isoleucine in ternary complexes of tripeptides with Cu(II) and 2,2′- bipyridine. *J. Mass Spectrom.* 2001; **36**: 306.
17. Lagarrigue M, Bossee A, Afonso C, Fournier F, Bellier B, Tabet JC. Diastereomeric differentiation of peptides with CuII and FeII complexation in an ion trap mass spectrometer. *J. Mass Spectrom.* 2006; **41**: 1073.
18. Zhang DX, Tao WA, Cooks RG. Chiral resolution of D- and L-amino acids by tandem mass spectrometry of Ni(II)-bound trimeric complexes. *Int. J. Mass Spectrom.* 2001; **204**: 159.
19. Bagheri-Majdi E, Ke YY, Orlova G, Chu IK, Hopkinson AC, Siu KWM. Copper-mediated peptide radical ions in the gas phase. *J. Phys. Chem. B* 2004; **108**: 11170.
20. Chu IK, Rodriquez CF, Lau TC, Hopkinson AC, Siu KWM. Molecular radical cations of oligopeptides. *J. Phys. Chem. B* 2000; **104**: 3393.
21. Barlow CK, Moran D, Radom L, McFadyen WD, O'Hair RAJ. Metal-mediated formation of gas-phase amino acid radical cations. *J. Phys. Chem. A* 2006; **110**: 8304.
22. Wee S, O'Hair RAJ, McFadyen WD. Side-chain radical losses from radical cations allows distinction of leucine and isoleucine residues in the isomeric peptides Gly-XXX-Arg. *Rapid. Commun. Mass Spectrom.* 2002; **16**: 884.
23. Lam CNW, Ruan EDL, Ma CY, Chu IK. Non-zwitterionic structures of aliphatic-only peptides mediated the formation and dissociation of gas phase radical cations. *J. Mass Spectrom.* 2006; **41**: 931.
24. Barlow CK, Wee S, McFadyen WD, O'Hair RAJ. Designing copper(II) ternary complexes to generate radical cations of peptides in the gas phase: Role of the auxiliary ligand. *Dalton Trans.* 2004; **20**: 3199.
25. Gatlin CL, Tureček F, Vaisar T. Copper(II) amino-acid complexes in the gas-phase. *J. Am. Chem. Soc.* 1995; **117**: 3637.
26. Gatlin CL, Tureček F, Vaisar T. Gas-phase complexes of amino-acids with Cu(II) and diimine ligands. 1. aliphatic and aromatic-amino-acids. *J. Mass Spectrom.* 1995; **30**: 1605.
27. Gatlin CL, Tureček F, Vaisar T. Gas-phase complexes of amino-acids with Cu(II) and diimine ligands. 2. amino-acids with o, n and s functional-groups in the side-chain. *J. Mass Spectrom.* 1995; **30**: 1617.
28. Gatlin CL, Rao RD, Turecek F, Vaisar T. Carboxylate and amine terminus directed fragmentations in gaseous dipeptide complexes with copper(II) and diimine ligands formed by electrospray. *Anal. Chem.* 1996; **68**: 263.
29. Vaisar T, Gatlin CL, Turecek F. Oxidation of peptide-copper complexes by alkali metal cations in the gas phase. *J. Am. Chem. Soc.* 1996; **118**: 5314.
30. Vaisar T, Gatlin CL, Turecek F. Metal-ligand redox reactions in gas-phase quaternary peptide-metal complexes by electrospray ionization mass spectrometry. *Int. J. Mass Spectrom. Ion Process.* 1997; **162**: 77.
31. Denekamp C, Rabkin E. Radical induced fragmentation of amino acids esters using triphenylcorrole (CuIII) complexes. *J. Am. Soc. Mass Spectrom.* 2007; **18**: 791.
32. Řehulka P, Popkov A, Nádvornik M, Planeta J, Mazanec K, Chmelik J. Off-line combination of reversed-phase liquid chromatography and laser desorption/ionization time-of-flight mass spectrometry with seamless post-source decay fragment ion analysis for characterization of square-planar nickel(II) complexes. *J. Mass Spectrom.* 2006; **41**: 448.
33. Kolářová L, Holčapek M, Jambor R, Dostál L, Nádvorník M, Růžička A. Structural analysis of 2,6-[bis(alkyloxy)methyl] phenyltin derivatives using electrospray ionization mass spectrometry. *J. Mass Spectrom.* 2004; **39**: 621.
34. Holčapek M, Kolářová L, Růžička A, Jambor R, Jandera P. Structural analysis of ionic organotin(IV) compounds using electrospray tandem mass spectrometry. *Anal. Chem.* 2006; **78**: 4210.
35. Jirásko R, Holčapek M, Kolářová L, Basu Baul TS. Electrospray ionization-multistage tandem mass spectrometry of complex multitin organometallic compounds. *J. Mass Spectrom.* 2007; **42**: 918.
36. Wei J, Chen J, Miller JM. Electrospray ionization mass spectrometry of organogermanium compounds. *Rapid. Commun. Mass Spectrom.* 2001; **15**: 169.
37. Ojanperä S, Pelander A, Pelzing M, Krebs I, Vuori E, Ojanperä I. Isotopic pattern and accurate mass determination in urine drug screening by liquid chromatography/time-of-flight mass spectrometry. *Rapid. Commun. Mass Spectrom.* 2006; **20**: 1161.
38. Lemr K, Holčapek M, Jandera P. Oxygen attachment to the metal complex ions during their collision induced dissociation in the ion trap. *Rapid Commun. Mass Spectrom.* 2000; **14**: 1878.

DOI: 10.1002/jms